PHYSICAL REVIEW C **78**, 011303(R) (2008)

$d_{5/2}$ proton hole strength in neutron-rich ^{43}P: Shell structure and nuclear shapes near $N = 28$

L. A. Riley,[1] P. Adrich,[2] T. R. Baugher,[1] D. Bazin,[2] B. A. Brown,[2,3] J. M. Cook,[2,3] P. D. Cottle,[4] C. Aa. Diget,[2] A. Gade,[2,3] D. A. Garland,[2,3] T. Glasmacher,[2,3] K. E. Hosier,[1] K. W. Kemper,[4] T. Otsuka,[3,5] W. D. M. Rae,[6] A. Ratkiewicz,[2,3] K. P. Siwek,[2,3] J. A. Tostevin,[7] Y. Utsuno,[8] and D. Weisshaar[2]

[1]*Department of Physics and Astronomy, Ursinus College, Collegeville, PA 19426, USA*
[2]*National Superconducting Cyclotron Laboratory, Michigan State University, East Lansing, MI 48824, USA*
[3]*Department of Physics and Astronomy, Michigan State University, East Lansing, MI 48824, USA*
[4]*Department of Physics, Florida State University, Tallahassee, FL 32306, USA*
[5]*Department of Physics and Center for Nuclear Study, University of Tokyo, Hongo, Tokyo 113-0033, Japan and RIKEN, Hirosawa, Wako-shi, Saitama 351-0198, Japan*
[6]*Garsington, Oxfordshire, OX44, United Kingdom*
[7]*Department of Physics, Faculty of Engineering and Physical Sciences, University of Surrey, Guildford, Surrey GU2 7XH, United Kingdom*
[8]*Advanced Science Research Center, Japan Atomic Energy Agency, Tokai, Ibaraki 319-1195, Japan*

(Received 4 June 2008; published 30 July 2008)

We report on the use of the one-proton knockout reaction from ^{44}S to determine the location of $d_{5/2}$ proton strength in neutron-rich ^{43}P. The results are used to test two shell-model frameworks with different pictures of the evolution of single-proton energies along the $N = 28$ isotones near the neutron dripline. We observe a concentration of $d_{5/2}$ proton hole strength near 1 MeV in excitation energy. This result favors the recent shell-model interaction of Utsuno *et al.* [Eur. Phys. J. Spec. Top. **150**, 187 (2007)] and provides additional evidence for an oblate shape for ^{42}Si.

DOI: 10.1103/PhysRevC.78.011303 PACS number(s): 24.50.+g, 21.10.Jx, 25.60.Gc, 27.40.+z

The nuclei in the vicinity of ^{42}Si have served as both a frontier for our understanding of the evolution of shell structure near the neutron dripline and a proving ground for the experimental techniques that will be used at the next generation of radioactive beam facilities. Whether major shell closures and magic numbers change at the neutron dripline and affect nuclear deformation is an open question that has generated a great deal of activity, and ^{42}Si has both $N = 28$—a major shell closure in stable nuclei—and a proton subshell closure ($Z = 14$) [1–3]. In addition to the $N = 28$ major shell closure being the lightest caused by the spin-orbit interaction, nuclei in the vicinity of ^{42}Si are among the heaviest isotopes near the neutron dripline that are accessible by the present generation of radioactive beam facilities, making them the best currently available subjects for the study of changing shell structure near the neutron dripline.

With new radioactive beam facilities being planned and constructed, there has been a tremendous effort to develop experimental tools that will allow detailed spectroscopic study of exotic isotopes produced at these new facilities. One of these tools is the one-nucleon knockout reaction with intermediate-energy beams. An effort to correlate cross sections measured with this reaction with theoretical cross sections, combining shell-model spectroscopic factors and single-particle cross sections from eikonal theory, is underway [4,5]. Analysis of the reaction presented here contributes to this effort. In the present Rapid Communication, we report on the use of the one-proton knockout reaction from ^{44}S to locate and quantify proton spectroscopic strength from the $d_{5/2}$ orbit in ^{43}P, which is one proton heavier than ^{42}Si. We find a concentration of $d_{5/2}$ proton hole strength near 1 MeV in excitation energy. This observation is reproduced by using shell-model calculations performed with the recently developed interaction of Utsuno *et al.* [6], which in turn supports an oblate shape for ^{42}Si.

The experiment was performed at the Coupled-Cyclotron Facility of the National Superconducting Cyclotron Laboratory at Michigan State University. The ^{44}S beam was produced by fragmentation of a 140 MeV/nucleon ^{48}Ca primary beam incident on a 705 mg/cm^2 ^{9}Be fragmentation target. The fragmentation products were separated in the A1900 fragment separator [7]. The secondary ^{44}S beam, with a purity of 81% and primary contaminant ^{45}Cl, was incident on a 376 mg/cm^2 thick ^{9}Be reaction target mounted at the target position of the S800 magnetic spectrograph [8]. The mid-target beam energy was 91.7 MeV/nucleon. A total of 9.3×10^8 incoming ^{44}S particles were well separated from contaminants by time of flight in scintillators mounted at the extended focal plane of the A1900 and at the object of the S800 analysis line. Projectile-like reaction products were identified by time of flight at the focal plane of the S800 and energy loss in the S800 ion chamber. The Segmented Germanium Array (SeGA) [9] of 32-fold segmented high-purity germanium detectors was used to detect γ rays emitted by excited reaction products.

The projectile-frame energy spectrum of γ rays measured in coincidence with ^{44}S beam particles and outgoing ^{43}P particles is shown in Fig. 1. A source velocity of $\beta = 0.405$ was used in the event-by-event Doppler correction of γ-ray energies measured in the laboratory frame. GEANT3 [10] simulations of the response of SeGA to γ rays were used to extract total γ-ray intensities from the measured spectrum. The measured spectrum was fitted with a linear combination of the simulated responseof the observed γ rays, the measured room background, and two exponential functions by using a log-likelihood maximization procedure. The exponential functions were included to account for the empirically observed prompt

 ©2008 The American Physical Society

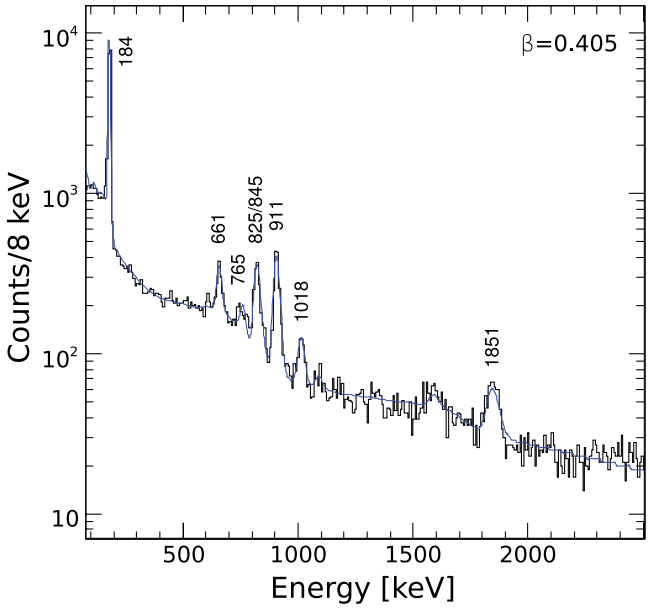

FIG. 1. (Color online) Doppler-corrected spectrum of γ rays measured in coincidence with recoiling ^{43}P particles. The solid curve is the GEANT3 fit described in the text.

component of the background. The resulting fit is shown as a solid curve in Fig. 1. In addition to the known [2,3] 184(1)-keV γ ray de-exciting the $J^\pi = \frac{3}{2}^+$ first excited state, six other γ rays are prominent in the spectrum at 661(4), 765(6), 825(5), 911(6), 1018(6), and 1851(11) keV. The 825- and 911-keV γ rays likely correspond to the 789(29)- and 918(26)-keV γ rays seen in the fragmentation study of Ref. [3]. In addition, the fitting process revealed that the peak at 825 keV is a doublet, containing a weak 845(4)-keV component.

Gamma-ray spectra measured in coincidence with the 184- and 825-keV γ rays are shown in the top and bottom panels

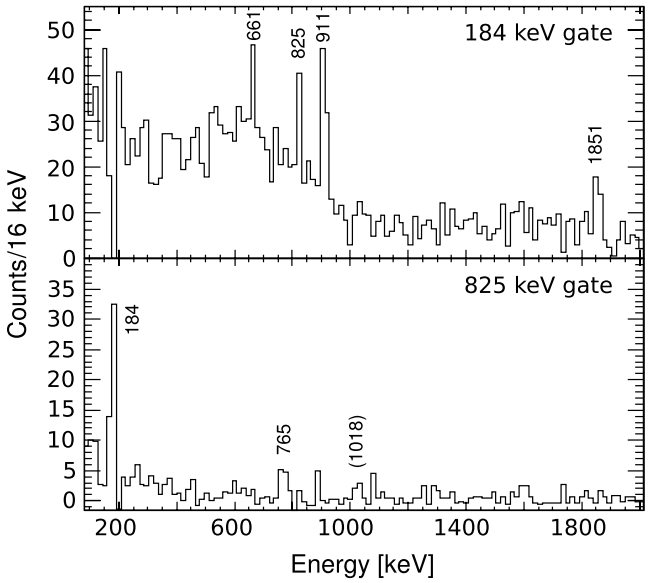

FIG. 2. Gamma-ray spectra measured in coincidence with the 184-keV (top panel) and 825-keV (bottom panel) γ rays.

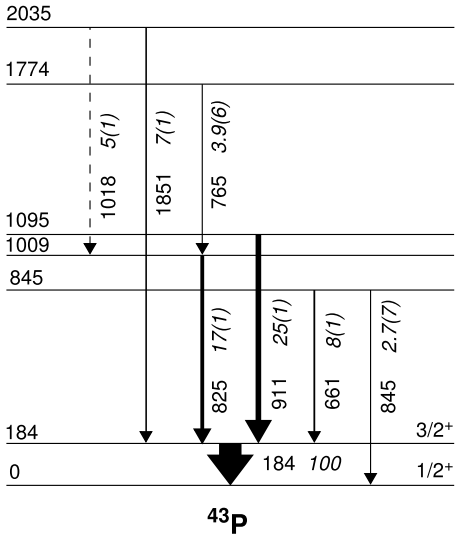

FIG. 3. Proposed level scheme of ^{43}P based on the present work. Gamma-ray intensities from the fitting process, relative to that of the 184-keV transition, appear in italics.

of Fig. 2. The 661-, 825-, 911-, and 1851-keV γ rays appear in the 184-keV gate spectrum. We observe no coincidences between these γ rays, so we place them directly atop the 184-keV $J^\pi = \frac{3}{2}^+$ first excited state in the proposed level scheme in Fig. 3. Although the apparent photopeak at 1018 keV in the 825-keV gate spectrum is not statistically significant, we tentatively place the 1018-keV transition above the 1009-keV state based on the energy difference between the 1009- and 2035-keV levels.

An inclusive single-proton knockout cross section $\sigma_{\rm inc} = 9.6(8)$ mb to bound final states of ^{43}P was determined from the number of outgoing ^{43}P reaction products relative to the number of incoming ^{44}S beam particles and the particle density of the reaction target. The uncertainty in the inclusive cross section includes the stability of the incoming beam (8%), the correction for the momentum acceptance of the S800 (3%), and the software gates used to select the reaction of interest (1%). Partial knockout cross sections to each level and the corresponding branching ratios appear in Table I. We discuss the consistency of these measured cross sections with theoretical predictions in the following. The inclusive cross

TABLE I. Excitation energies, spins and parities J^π, single-particle configurations nlj, measured knockout branching ratios BR, measured partial cross sections σ, and single-particle cross sections $\sigma_{\rm sp}$ from reaction theory.

$E_{\rm level}$ (keV)	J^π ($\hbar$)	nlj	BR (%)	σ (mb)	$\sigma_{\rm sp}$ (mb)
0	$1/2^+$	$2s_{1/2}$	24(4)	2.3(4)	8.37
184	$3/2^+$	$1d_{3/2}$	33(2)	3.1(3)	7.00
845	$(5/2^+)$	$(1d_{5/2})$	4(1)	0.37(7)	7.73
1009	$(5/2^+)$	$1d_{(5/2)}$	8(2)	0.8(2)	7.70
1095	$(5/2^+)$	$1d_{(5/2)}$	20(1)	1.9(2)	7.68
1774	$(5/2^+)$	$(1d_{5/2})$	4(1)	0.4(1)	7.55
2035	$(5/2^+)$	$(1d_{5/2})$	7(2)	0.7(2)	7.50

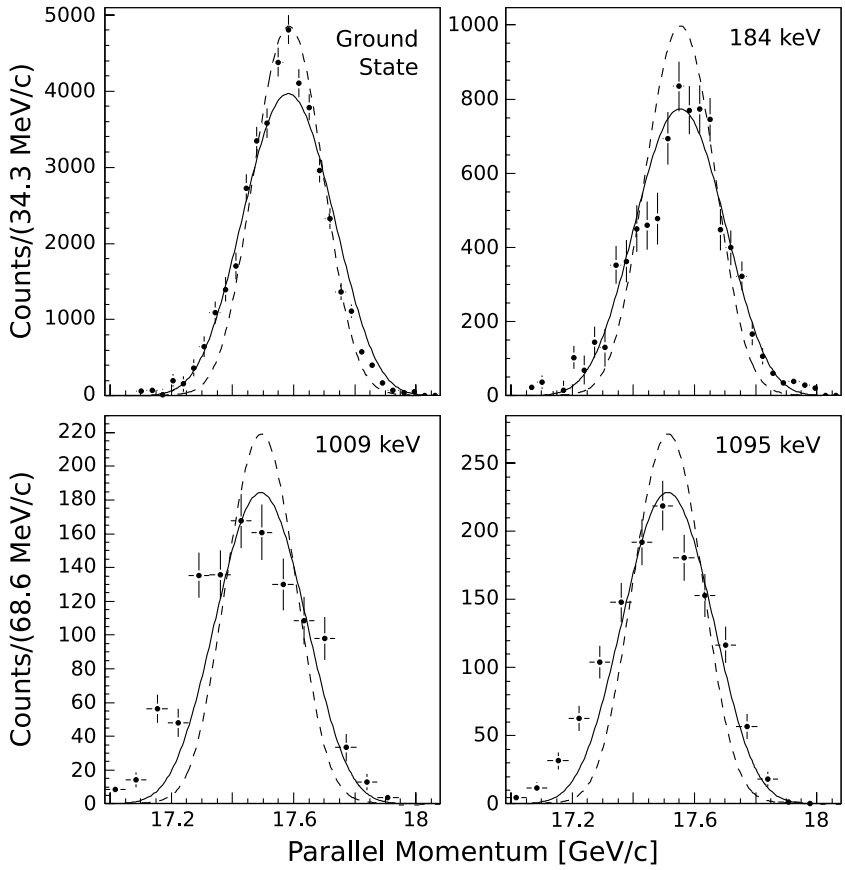

FIG. 4. Parallel momentum distributions of states of ^{43}P populated in one-proton knockout from ^{44}S. The curves are theoretical distributions, described in the text, for $l = 0$ (dashed) and $l = 2$ (solid).

section from the present experiment is in agreement with that obtained in the earlier one-proton knockout measurement of Fridmann *et al.* [2]. The prior measurement was made with a reaction target of the same thickness but with a factor of 85 fewer beam particles. In the prior work, only the 184-keV transition was observed at a level of 75(15)% of the inclusive cross section. If we do not correct for feeding from higher lying states, the knockout branching ratio of the 184-keV level from the present work is 73(4)%, in excellent agreement with the earlier result.

Parallel momentum distributions of ^{43}P reaction residues in the ground state and the strongly populated excited states at 184, 1009, and 1095 keV are shown in Fig. 4. The excited-state distributions were obtained by gating on the de-excitation γ rays identified at the upper right in each panel in the figure. The distribution of the first excited state was corrected for feeding by the 825- and 911-keV transitions based on the measured γ-ray intensities. The ground-state distribution was obtained with a linear combination of distributions measured in coincidence and in anticoincidence with γ rays as described in Ref. [11].

The curves in Fig. 4 are eikonal-model calculations produced by using the method described in Ref. [5]. The incoming beam was not monoenergetic, so the measured momentum distribution of the unreacted ^{44}S beam has been folded into the theoretical distributions. In addition, the incoming ^{44}S beam particles lose more energy per unit target thickness than the ^{43}P reaction products. In our measurement, the different energy losses of incoming and outgoing particles contributed $\frac{\Delta p}{p} = 0.8\%$ to the momentum spread of the ^{43}P particles. A rectangular distribution of this width has also been folded into the theoretical distributions.

The dashed curves in Fig. 4 correspond to removal of a proton with orbital angular momentum $l = 0$ and separation energy 22.2 MeV, and the solid curves correspond to $l = 2$. The measured distributions show a small asymmetry, having low momentum "tails." This phenomenon has been observed in several cases [11–14]. Except for very weakly bound systems [15], it is not well understood, but it is thought to arise from a dissipative mechanism not accounted for by eikonal theory [13]. To avoid bias from the low-momentum tails, we have fitted the theoretical distributions in Fig. 4 to the measured cross sections above 17.4 GeV/c. Above this value, the momentum distributions of the three excited states are compatible with $l = 2$ and the ground state with $l = 0$ distributions. These l assignments suggest a $\pi s_{1/2}$ configuration in the ground state and $\pi d_{3/2}$ configuration for the first excited state, compatible with prior J^π assignments of $1/2^+$ and $3/2^+$ to these states. The assignment of $l = 2$ to the excited states at 1009 and 1095 keV, along with energies significantly above the first excited state, is consistent with their interpretation as arising from the removal of a proton from the more deeply bound $d_{5/2}$ proton orbital in ^{44}S.

As described in Ref. [16], the theoretical cross section for populating a final state identified by nJ^π is calculated by combining the single-particle cross section $\sigma_{\rm sp}(nJ^\pi)$ from

eikonal-model calculations with the shell-model spectroscopic factor C^2S:

$$\sigma_{\rm th}(nJ^\pi) = \left(\frac{A}{A-1}\right)^N C^2S\,\sigma_{\rm sp}(l, B_n), \qquad (1)$$

where N is the oscillator quantum number, l is the angular momentum, and B_n is the binding energy of the orbital from which the nucleon is removed.

Our understanding of single-particle occupancies has evolved over the past decade through $(e, e'p)$ measurements on stable nuclei and single-nucleon knockout reactions on exotic isotopes. These experiments demonstrate that the classical single-particle model picture of fully occupied, deeply bound single-particle states requires modification because of several correlation effects. These correlation effects are quantified with a "reduction factor" R_s obtained from experimental and theoretical inclusive knockout cross sections via [4]

$$R_s = \frac{\sigma_{\rm exp}^{\rm inc}}{\sum_{nJ^\pi}\sigma_{\rm th}(nJ^\pi)}, \qquad (2)$$

where the sum includes all shell-model states below the nucleon separation energy. Single-nucleon knockout studies have mapped the systematics of the dependence of the required reduction on the difference between the energies of the neutron and proton Fermi surfaces. In a recent article, Gade *et al.* [17] present a plot of reduction factors from several single-nucleon knockout studies versus the difference ΔS in proton and neutron separation energies; their plot shows a well-defined systematic dependence. In short, the reduction factor is small (with observed values as low as 0.25) when the knocked-out nucleon is tightly bound and large (approaching 1.0) when the knocked-out nucleon is loosely bound. For ^{44}S, the incident exotic nucleus in the present study, ΔS is 17(1) MeV. A weighted least-squares fit to the reduction factor plot in Ref. [17] with this difference in binding energies gives $R_s = 0.33(3)$ for the present proton knockout reaction. This is identical to the result reported in the following, which we obtain from Eq. (2).

In the upper left panel of Fig. 5, measured cross sections for the states in ^{43}P observed here, and believed to have $J^\pi = 5/2^+$, are shown in bins corresponding to 250-keV intervals in excitation energy. Two sets of shell-model calculations [18] were combined with the eikonal single-particle cross sections via Eq. (1) to calculate the theoretical cross sections shown in the two lower right panels of the figure. The first set, labeled Nowacki-01 (lower panel), is performed with the interaction used in Ref. [19] in which the effective spin-orbit $\pi d_{3/2}$-$\pi d_{5/2}$ splitting is 5.9 MeV in ^{48}Ca and 6.6 MeV in ^{42}Si. In the second set, labeled Utsuno-08 (center panel), we show results based on a new effective interaction for this mass region, described in Refs. [20] and [6], that takes into account some empirical trends observed for the effective central and tensor components of the interactions for the *sd* [21] and *pf* [22,23] shells. For Utsuno-08 the effective $\pi d_{3/2}$-$\pi d_{5/2}$ spin-orbit splitting is 5.2 MeV in ^{48}Ca and 6.5 MeV in ^{42}Si. The numerical values in the two lower left panels of Fig. 5 are the shell-model spectroscopic factors. The theoretical cross sections in Fig. 5

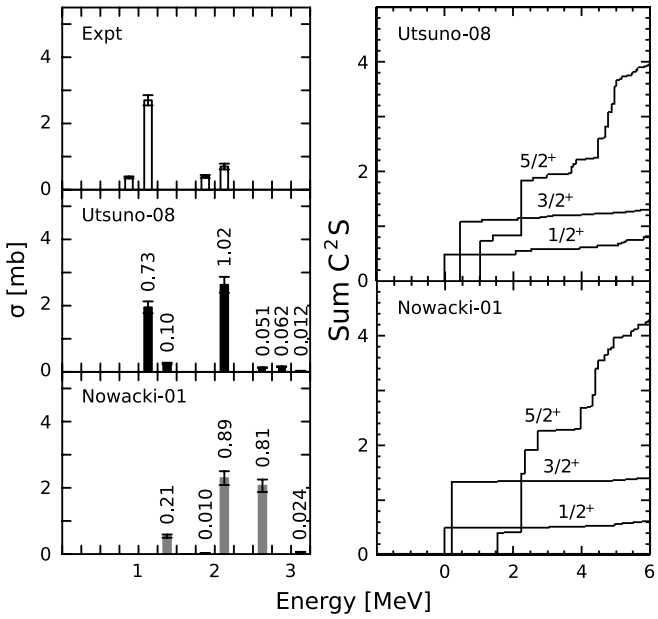

FIG. 5. Measured partial knockout cross sections to $J^\pi = 5/2^+$ states below the neutron separation energy (top left panel) in 250-keV bins compared with theoretical cross sections (two bottom right panels) described in the text. The numerical values in the two bottom left panels are the shell-model spectroscopic factors C^2S. The plots on the left show spectroscopic factors summed as a function of excitation energy up to 6 MeV for each spin.

have been scaled by the reduction factor $R_s = 0.33(3)$ obtained by using Eq. (2) when using the theoretical cross sections based on the shell-model calculations with the Utsuno-08 interaction. The error bars on the theoretical cross sections in the figure reflect the uncertainty in the reduction factor. The main difference between the calculations based on the two shell-model interactions is that the Utsuno-08 gives more $d_{5/2}$ strength near 1.1 MeV, in better agreement with experiment. The strength near 2 MeV is too large with both interactions. This shows the sensitivity of these measurements to the interactions. The right side of the figure shows the shell-model spectroscopic factors summed as a function of excitation energy up to 6 MeV for each spin (which requires about 50 states for each spin). The present experiment is sensitive to the strength below 3 MeV, which contains 51% (45%) of the total *sd*-shell sum-rule strength of 8 with the Nowacki-01 (Utsuno-08) interaction. The fraction of the sum rule up to 6 MeV is 82% (76%). These results nicely show the large fractionation of spectroscopic strength that occurs in mid-shell nuclei and how its distribution reflects both the single-particle and collective properties of the nucleus.

The shape of ^{42}Si has been the subject of considerable discussion during the past several years. At first, it was expected that this nucleus would be spherical because of its neutron number, 28, which is magic along the line of stability, and its $Z = 14$ subshell closure. However, shell structure is much less certain near the neutron dripline, and the shape of ^{42}Si has been the topic of debate. Much of the discussion has been centered on the role of the neutron orbits in determining the shape of ^{42}Si and its neighbors. It was predicted [24,25]

that the spin-orbit force affecting neutron orbits weakens close to the neutron dripline because of both the weak binding of neutrons and the role of the continuum. More specifically, a number of authors have predicted that the $N = 28$ shell closure narrows or even collapses as protons are removed from the doubly-magic nucleus ^{48}Ca [26–33], causing the deformation of ^{42}Si. In contrast, it was argued in Ref. [34] that the proton-subshell closure at $Z = 14$ would be a strong stabilizing influence, hindering deformation and maintaining a spherical shape.

The accumulating experimental evidence on ^{42}Si has not yet fully clarified the situation. A measurement of the β decay of ^{42}Si was used to argue for a deformed shape for this nucleus [1], as was the observation that ^{43}Si is bound [35]. The measurement of a small cross section for two-proton knockout from ^{44}S was interpreted as evidence for the persistence of the $Z = 14$ subshell closure in ^{42}Si, which would favor a spherical shape [2]. Mass measurements of Cl, S, and P isotopes in the region [36] indicate a weakening of the $N = 28$ shell for $Z > 14$, but the mass measurement of ^{42}Si [37] is inconclusive, the result being consistent with either a spherical or deformed shape. Most recently, the fragmentation study of Bastin *et al.* [3] revealed a low-lying excited state of ^{42}Si (presumed to have $J^{\pi} = 2^{+}$) at 770(19) keV, and inverse kinematics proton scattering from ^{40}Si [38] showed a low 2^{+}_{1} energy and enhanced collectivity relative to mid-shell, both strongly suggestive of a reduced $N = 28$ shell gap and a deformed shape at $Z = 14$. The lowering of $\pi d_{5/2}$ strength is correlated with a lowering of the 2^{+} energy in ^{42}Si from 1.49 MeV with Nowacki-01 to 0.87 MeV with Utsuno-08, to be compared with the recent experimental value of 0.77 MeV [3]. The result reported here for the distribution of $d_{5/2}$ proton hole strength in ^{43}P, with its agreement with the shell-model calculation of Ref. [6], adds to the supporting evidence for an oblate shape in ^{42}Si.

In summary, we have reported on the use of the one-proton knockout reaction from ^{44}S to identify $d_{5/2}$ proton hole strength in neutron-rich ^{43}P. The results have been used to test two shell-model interactions, of which only one—that of Ref. [6]—can reproduce the concentration of $d_{5/2}$ strength near 1 MeV. This lends support to the growing evidence that ^{42}Si has an oblate shape.

This work was supported by the National Science Foundation under Grant Nos. PHY-0606007, PHY-0355129, PHY-0653323, and PHY-0555366 and by the United Kingdom Science and Technology Facilities Council (STFC) under Grant No. EP/D003628. YU acknowledges support from the JSPS core-to core project, EFES, and Grant-in-Aid for Young Scientists (17740165) from MEXT.

[1] S. Grévy *et al.*, Phys. Lett. **B594**, 252 (2004).
[2] J. Fridmann *et al.*, Nature (London) **435**, 922 (2005); J. Fridmann *et al.*, Phys. Rev. C **74**, 034313 (2006).
[3] B. Bastin *et al.*, Phys. Rev. Lett. **99**, 022503 (2007).
[4] B. A. Brown, P. G. Hansen, B. M. Sherrill, and J. A. Tostevin, Phys. Rev. C **65**, 061601 (2002).
[5] P. G. Hansen and J. A. Tostevin, Annu. Rev. Nucl. Part. Sci. **53**, 219 (2003).
[6] Y. Utsuno, T. Otsuka, T. Mizusaki, and M. Honma, Eur. Phys. J. Spec. Top. **150**, 187 (2007).
[7] D. J. Morrissey *et al.*, Nucl. Instrum. Methods Phys. Res. B **204**, 90 (2003).
[8] D. Bazin *et al.*, Nucl. Instrum. Methods Phys. Res. B **204**, 629 (2003).
[9] W. F. Mueller *et al.*, Nucl. Instrum. Methods Phys. Res. A **466**, 492 (2001).
[10] GEANT version 3.21, CERN program library, long writeup W5013 (1994).
[11] A. Gade *et al.*, Phys. Rev. C **69**, 034311 (2004).
[12] J. Enders *et al.*, Phys. Rev. C **65**, 034318 (2002).
[13] A. Gade *et al.*, Phys. Rev. C **71**, 051301(R) (2005).
[14] J. R. Terry *et al.*, Phys. Rev. C **77**, 014316 (2008).
[15] J. A. Tostevin *et al.*, Phys. Rev. C **66**, 024607 (2002).
[16] J. R. Terry *et al.*, Phys. Rev. C **69**, 054306 (2004).
[17] A. Gade *et al.*, Phys. Rev. C **77**, 044306 (2008).
[18] B. A. Brown and W. D. M. Rae, NuShellX, http://www.nscl.msu.edu/∼brown/resources/resources.html; http://knollhouse.org/default.aspx.
[19] S. Nummela *et al.*, Phys. Rev. C **63**, 044316 (2001).
[20] T. Otsuka, T. Suzuki, R. Fujimoto, H. Grawe, and Y. Akaishi, Phys. Rev. Lett. **95**, 232502 (2005).
[21] B. A. Brown and W. A. Richter, Phys. Rev. C **74**, 034315 (2006).
[22] W. A. Richter, M. G. van der Merwe, R. E. Julies, and B. A. Brown, Nucl. Phys. **A523**, 325 (1991).
[23] M. Honma, T. Otsuka, B. A. Brown, and T. Mizusaki, Eur. Phys. J. A **25**, Suppl. 1, 499 (2005).
[24] W. Nazarewicz and R. F. Casten, Nucl. Phys. **A682**, 295c (2001).
[25] D. Warner, Nature (London) **430**, 517 (2004).
[26] T. R. Werner *et al.*, Phys. Lett. **B333**, 303 (1994).
[27] T. R. Werner *et al.*, Nucl. Phys. A **597**, 327 (1996).
[28] J. Terasaki, H. Flocard, P.-H. Heenen, and P. Bonche, Nucl. Phys. **A621**, 706 (1997).
[29] G. A. Lalazissis, A. R. Farhan, and M. M. Sharma, Nucl. Phys. **A628**, 221 (1998).
[30] G. A. Lalazissis, D. Vretenar, P. Ring, M. Stoitsov, and L. Robledo, Phys. Rev. C **60**, 014310 (1999).
[31] S. Péru, M. Girod, and J. F. Berger, Eur. Phys. J. A **9**, 35 (2000).
[32] R. Rodríguez-Guzmán, J. L. Egido, and L. M. Robledo, Phys. Rev. C **65**, 024304 (2002).
[33] J. Piekarewicz, J. Phys. G **34**, 467 (2007).
[34] P. D. Cottle and K. W. Kemper, Phys. Rev. C **58**, 3761 (1998).
[35] M. Notani *et al.*, Phys. Lett. **B542**, 49 (2002).
[36] F. Sarazin *et al.*, Phys. Rev. Lett. **84**, 5062 (2000).
[37] B. Jurado *et al.*, Phys. Lett. **B649**, 43 (2007).
[38] C. M. Campbell *et al.*, Phys. Rev. Lett. **97**, 112501 (2006); C. M. Campbell *et al.*, Phys. Lett. **B652**, 169 (2007).